Chemically selective modification of spin polarization in ultrathin ferromagnetic films: Microscopic theory and macroscopic experiment

K. P. Kopper, D. Küpper, R. Reeve, and T. Mitrelias
Cavendish Laboratory, University of Cambridge, J. J. Thomson Avenue, Cambridge CB3 0HE, United Kingdom

D. S. D. Gunn and Stephen J. Jenkins
Department of Chemistry, University of Cambridge, Lensfield Road, Cambridge CB2 1EW, United Kingdom

(Received 18 January 2009; revised manuscript received 4 August 2009; published 31 August 2009)

Modulation of thin-film magnetic properties will be key to the design of future magnetoelectronic (spintronic) devices. Here, we report the influence of atomic adsorbates upon ultrathin cobalt films on copper, employing secondary electron spin polarization as an incisive experimental probe. We observe that nitrogen suppresses measured polarization by ~20% for the thickest layers; oxygen has little impact in this regime. Moreover, we develop a model capable of predicting these effects, forging a crucial link between microscopic theory and an observable macroscopic magnetic phenomenon.

DOI: 10.1103/PhysRevB.80.052406 PACS number(s): 75.70.Rf, 71.15.Mb, 75.50.Cc, 75.70.Ak

The properties of ferromagnetic thin films continue to elicit considerable interest among both the pure and applied magnetism research communities.[1] From a fundamental perspective, their properties provide an opportunity to examine the effects of reduced dimensionality and reduced effective atomic coordination upon magnetic phenomena; while for the designer of magnetoelectronic (spintronic) devices, those same effects provide novel opportunities, ripe for exploitation.[2] Whichever viewpoint is taken, controllable modification of thin-film magnetic properties is a key target for current research.

Among possible routes for such manipulation, the effect of adsorbed species exerts a lasting fascination. Both theory and experiment have long suggested that adsorbates such as CO can drastically alter the magnetic properties of surfaces and thin films, both microscopically (for example, the quenching of spin moments in the surface layers of iron,[3–10] cobalt[10–12] or nickel[10,13–16]) and/or macroscopically (as in the spin-reorientation transitions observed within thin-films of cobalt or nickel[17–20]). Yet the connection between the calculation of microscopic changes in spin moments and experimentally observed changes in macroscopic magnetic properties is rarely obvious. One intention of the present work is to forge a link between the theoretical description of adsorbate-induced magnetic modification and results obtained via an incisive experimental probe.

To this end, we have investigated the change in secondary electron spin polarization (SESP) as a function of Co thickness for nitrogen and oxygen adsorption on Co/Cu{100}. To measure the SESP of these systems experimentally, we have used a highly sensitive secondary electron spin polarimeter. Theoretically, we propose a model that generates SESP values from our density functional theory (DFT) data thus enabling for the first time a direct comparison between theory and experiment.

The experimental system comprises a compact *in situ* 25 kV retarding potential spin polarimeter (see Ref. 21) as the main scientific instrument, together with standard surface science equipment such as a combined four-grid low energy electron diffraction (LEED) and Auger electron spectroscopy (AES) system, a sputtering gun and electron beam evaporators. The Cu{100} single crystal was cleaned with repeated Ar^+-ion sputtering—annealing cycles and cobalt films were evaporated from a high purity (99.995%) cobalt rod, at pressures below 5×10^{-10} mbar and deposition rates between 0.5 and 0.7 ML/min.

In order to accurately and reproducibly control the adsorbate on the Co thin film, considerable attention was paid to gas-induced changes in the periodicity of the Cu{100} surface. Oxygen was preadsorbed by exposing the substrate to 2500 L ($1\ \mathrm{L}=1\times10^{-6}$ Torr s) of 99.9995% O_2 at the elevated temperature of 515 K. Oxygen dissociates and a $(\sqrt{2}\times2\sqrt{2})\mathrm{R}45°$-O reconstructed Cu{100} surface results. The O adatoms are known to occupy fourfold hollow sites[22] and the surface coverage is $\theta=0.5$ ML.[22,23] Similarly, 0.5 ML[24] of N was preadsorbed on Cu by ionizing 99.9995% N_2 and exposing the substrate to the accelerated N^+ ions,[25] followed by annealing to 625 K. A $c(2\times2)$ LEED pattern is observed, with N adatoms occupying fourfold hollow sites.[24] In both cases excess amounts of gas are applied, the surface saturates naturally, and the adsorbed quantity of 0.5 ML O/N adatoms is determined by observation of the surface periodicity.[25] Following the preparation of the O-and N-treated Cu surface, Co was incrementally deposited and the corresponding room-temperature SESP measured, while surface morphology as well as chemical composition were monitored with LEED and AES, respectively.

The $c(2\times2)$ patterns observed in LEED after cobalt deposition onto the N-and O-covered copper surfaces are characteristic for N (Ref. 26) and O adatoms[27] adsorbed to fcc Co{100} and indicate that both species have changed substrate, remaining at the vacuum interface during film growth. AES measurements confirm that the adsorbed quantity of gas is constant during change of substrate from Cu to Co, and corresponds to 0.5 ML.[25,28] Secondary electrons are excited by primary electrons of 1 keV (Ref. 25) and the measured polarization arises from emitted electrons with secondary energies from zero to the primary excitation energy. The evolution of the SESP with Co thickness provides the reference against which the spin polarization of the gas-adsorbed surface is compared. In all measurements the external magnetic field was aligned along a ⟨100⟩ direction. Figure 1(a) shows a comparison between the polarization originating from the

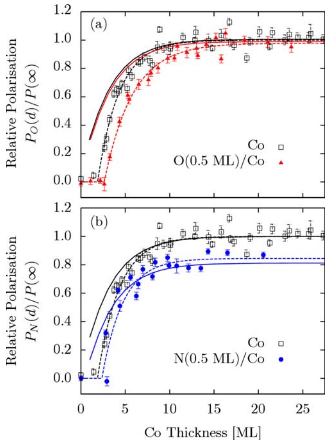

FIG. 1. (Color online) The relative SESP as a function of Co thickness is shown; values for the clean cobalt film are represented by open squares; those for the 0.5 ML O-covered surface are depicted as triangles; and those for the 0.5 ML N-covered surface are depicted as circles. Dotted (solid) lines represent the experimental (theoretical) fit, with black for the clean surface, and red (gray) for the O-covered surface in (a) and blue (gray) for the N-covered surface in (b).

clean Co film and that obtained from the Co film covered with 0.5 ML of O adatoms. For easy comparison of the clean, oxygen and nitrogen data the relative polarization $P_k(d)/P(\infty)$ is plotted, where $P(\infty)$ denotes the asymptotic polarization of the clean cobalt surface and k is used to indicate the adsorbate species (if any). The function

$$P_k(d) = P_k(\infty)\left(1 - \exp\left[-\frac{d - d_k^{fm}}{\lambda_k^{eff}}\right]\right), \qquad (1)$$

describes the data for films of thickness, d, greater than the room-temperature ferromagnetic phase transition thickness (d_k^{fm}). Besides d_k^{fm}, fitting Eq. (1) to the data yields the asymptotic polarization, $P_k(\infty)$, and the experimentally obtained effective information depth (λ_k^{eff}). Equation (1) accounts for an exponential decay of the signal with the depth of the emitting atom, by analogy with other electron spectroscopy techniques such as AES.[29,30] Specifically, this form was derived by assuming that the *total* number of secondary electrons emitted is independent of the thickness of the Co film (reasonable, given the proximity of Co and Cu in the periodic table) and that the variation of polarization with film thickness therefore derives purely from the *difference* in the numbers of emitted spin up and spin down electrons. Making the simplest possible assumption, namely, that the absolute spin asymmetry in the numbers of generated secondary electrons is constant in each Co layer (and zero in each Cu layer) we need only apply an exponential attenuation factor and integrate to achieve Eq. (1) in the case where d_k^{fm} is zero; the latter parameter is then inserted in an *ad-hoc* manner to mimic depression of the Curie temperature for the thinnest films by simply treating the first few Co layers as nonferromagnetic. The room-temperature ferromagnetic phase transition thickness, d_k^{fm}, obtained from the clean Co film was found to be 1.6 ± 0.2 ML, in good agreement with values reported in the literature ranging from 1.3 ± 0.3 ML (Ref. 31) to 1.6 ± 0.3 ML,[32] validating both experimental and data analysis methods. For the bare Co film an asymptotic polarization of $P(\infty) = 7.6 \pm 0.1\%$ was found. The presence of 0.5 ML of adsorbed O adatoms barely changes the asymptotic polarization to $98 \pm 2\%$ of the value obtained for the clean surface, which amounts to $P_O(\infty) = 7.4 \pm 0.1\%$. However, we find the ferromagnetic phase transition thickness to be increased by approximately 1 ML. Figure 1(b) shows Co deposited on the nitrogen-preadsorbed surface, again in comparison to the clean Co film. The 0.5 ML of adsorbed N adatoms reduces the asymptotic polarization significantly to $P_N(\infty) = 6.3 \pm 0.2\%$, or $84 \pm 3\%$ compared to the bare film. Similarly to adsorbed oxygen, we find the onset of ferromagnetism delayed by about 1 ML.

Our experimental data thus quantifies the change in the SESP of Co/Cu{100} surfaces upon oxygen and nitrogen adsorption, but these experiments alone are unable to clarify precisely the principles behind this effect. In the remainder of this Brief Report, we use theoretical calculations to elucidate the nature of the SESP suppression in a unique opportunity to merge experimental and theoretical data.

The CASTEP computer code[33] was used for all of the calculations in this work. Ultrasoft pseudopotentials[34] and a plane-wave cutoff energy of 340 eV were used throughout, along with the generalized gradient approximation (GGA) in the Perdew-Wang form.[35] All of the calculations were spin polarized, necessitating the Co pseudopotentials to include nonlinear core-corrections (NLCC) (Ref. 36) for an accurate description of the magnetism. Bader's method of topological analysis[37] was implemented to resolve spin magnetic moments at an atomic level.

The system was modeled using a supercell containing six Cu layers upon which 1–6 ML of Co was added, along with either O or N atoms for each Co coverage. The 0.5 ML gas-adsorbed surfaces were modeled with a $c(2\times2)$ arrangement of adatoms in a $p(2\times2)$ unit cell containing a vacuum region of over 15 Å and with the Brillouin zone sampled using a $4\times4\times1$ Monkhorst-Pack[38] **k**-point mesh. The adsorbates were modeled in the fourfold hollow site only, as this is well-established from experimental data on Co{100}.[26,27] The bare surfaces (i.e., 1–6 ML Co overlayers with no adsorbate) were studied under identical methodological conditions to avoid numerical discrepancies. For all calculations, adsorption was allowed on only one side of the slab, and the bottom four Cu layers were held in an ideal fixed geometry with the remainder of the system allowed to relax according to the calculated forces. In all cases, the lateral dimensions of the supercell were held at the Cu lattice constant, emulating the epitaxial growth of Co on the Cu surface.

Initially, the calculations provide us with values of the spin magnetic moment for each of the atoms present, which is not a property that is directly comparable to the experimentally measured SESP. From this raw data, therefore, we generate values for the number of spin up and spin down valence electrons on each atom as a precursor to the calculation of a *theoretical* SESP. We simplify somewhat by noting that the various layers can be broadly categorized as falling into five basic groups whose spin properties are only weakly dependent upon the film thickness. These basic groups are labeled as: "Cu" for all Cu layers; "inter" for the

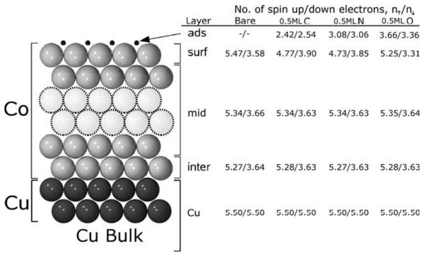

No. of spin up/down electrons, $n_\uparrow/n_\downarrow$

Layer	Bare	0.5ML C	0.5ML N	0.5ML O
ads	-/-	2.42/2.54	3.08/3.06	3.66/3.36
surf	5.47/3.58	4.77/3.90	4.73/3.85	5.25/3.31
mid	5.34/3.66	5.34/3.63	5.34/3.63	5.35/3.64
inter	5.27/3.64	5.28/3.63	5.27/3.63	5.28/3.63
Cu	5.50/5.50	5.50/5.50	5.50/5.50	5.50/5.50

FIG. 2. Layer classification with included table showing the average number of spin up and down valence electrons per atom in these layers.

interface Co layer adjacent to the uppermost Cu layer; "mid" for the middling Co layers; "surf" for the surface Co layer; "ads" for the adsorbate layer (Fig. 2). We evaluate these for a film thickness of 6 ML, where the values are sufficiently converged to allow extrapolation of the model to greater thicknesses not covered directly by the DFT calculations.

Having thus obtained the parameterized valence spin polarization, we are now in a position to calculate the total attenuated values for the spin up ($N_\uparrow^d$) and spin down ($N_\downarrow^d$) secondary valence electrons that are emitted,

$$N_\uparrow^d = \sum_{i=1}^{\infty} n_\uparrow^d(i) e^{-(i-1)/\lambda}; \quad N_\downarrow^d = \sum_{i=1}^{\infty} n_\downarrow^d(i) e^{-(i-1)/\lambda}, \tag{2}$$

where $n_\uparrow^d(i)$ is the average number [as evaluated over the $p(2\times 2)$ cell] of spin up valence electrons per atom in the ith layer of the material (such that $i=1$ is the surface layer) for a given Co film thickness, d; $n_\downarrow^d(i)$ is the equivalent for the spin down valence electrons; λ represents the effective attenuation length for these secondary electrons, and is chosen to have a value of 3 ML.[25]

The model used to determine the theoretical SESP of a bare Co/Cu{100} surface is then given by Eq. (3), where N_0 is an adjustable parameter that represents an unknown number of unpolarized electrons emitted from core states,

$$P(d) = \frac{N_\uparrow^d - N_\downarrow^d}{N_\uparrow^d + N_\downarrow^d + N_0}. \tag{3}$$

Ignoring the effect of unpolarized electrons results in a value of the calculated SESP much higher than that found experimentally. For example, if we were to evaluate the theoretical asymptotic SESP of Co on our Cu{100} surface setting $N_0 = 0$, we obtain a value of approximately 20%, which does not match at all well with the experimental value (7.6%). In the real system, the measured SESP signal is diluted by a large number of unpolarized electrons emitted from core states. We fit a value of $N_0=49$ to obtain a theoretical asymptotic SESP of 7.6% for the clean Co film.[25] Note that N_0 is considered to be independent of film thickness, since we assume that emission from core states is probably similar from Co and Cu atoms. The choice of N_0 modifies slightly the precise shape of modeled SESP curves, but its main effect is in scaling the result to ensure that the asymptotic SESP is reproduced correctly. The sum ($N_\uparrow^d + N_\downarrow^d$) varies only relatively weakly with the number of Co layers, compared with the more sensitive difference ($N_\uparrow^d - N_\downarrow^d$). In the limit of a very thick clean Co overlayer, the denominator in Eq. (3) asymptotically approaches a value of ~80.79 (i.e., the contribution from core states accounts for approximately 61% of the total secondary electron yield), while the numerator approaches a value of ~6.13.

TABLE I. Experimental and theoretical asymptotic polarization values for Co/Cu{100} surfaces. All values are expressed as percentages. Error estimates for theoretical figures are justified in the supporting material (Ref. 25).

	Experiment		Theory	
k	$P_k(\infty)$	$P_k(\infty)/P(\infty)$	$P_k(\infty)$	$P_k(\infty)/P(\infty)$
	7.6 (±0.1)	100	7.6	100
O	7.4 (±0.1)	98 (±2)	7.6 (±0.1)	100 (±1)
N	6.4 (±0.2)	84 (±3)	6.2 (±0.4)	81 (±6)
C			6.1 (±0.5)	81 (±6)

Once N_0 is determined for the clean film, we then assume it remains unaltered for adsorbate-covered surfaces. For the O- and N-covered surfaces, the adsorbate electrons are treated as part of the surface layer, and are therefore unattenuated (but weighted by the fractional coverage, θ_k),

$$P_k(d) = \frac{N_\uparrow^d - N_\downarrow^d + (n_\uparrow^{ads} - n_\downarrow^{ads})\theta_k}{N_\uparrow^d + N_\downarrow^d + N_0 + (n_\uparrow^{ads} + n_\downarrow^{ads} + n_0^{ads})\theta_k}, \tag{4}$$

where $n_0^{ads}=2$ accounts for the core electrons in the adatoms.

Application of this model generates the theoretical curves displayed in Fig. 1; the asymptotic values of SESP are shown in Table I. We can see that the experimental and theoretical values for the SESP of adsorbate-covered systems show excellent agreement for the thickest films (i.e., for thicknesses that give a relative polarization close to the asymptotic value), while there remains some disparity at the lower thicknesses. Oxygen adsorption has only a very minor effect on the asymptotic SESP, whereas nitrogen suppresses this polarization to a far greater extent.

Despite such close agreement between experiment and theory for the thickest films studied, it is notable that the results diverge markedly below around 10 ML. We believe that this is due to a thermal effect: Curie temperatures are known to be suppressed in ultrathin films,[39] and while the experiments here were carried out at 300 K, the DFT calculations provide strictly 0 K results. To some degree, the separation between experimental and theoretical SESP curves in Fig. 1 may therefore be interpreted as a measure of thermal spin suppression for the thinnest films. Repetition of the experiments at lower temperature would be highly desirable, but would require a redesign of the sample manipulator.

We might also reasonably ask whether the simplification of parameterizing the DFT data (rather than using the raw values) results in a significant deviation in the theoretical SESP? The answer is no (at least up to the calculated 6 ML coverage), with the single exception of 1 ML Co coverage in the N-adsorbed system. Here, the raw DFT calculations actually result in an antiferromagnetic solution within the Co film. The otherwise close agreement in the ultrathin regime supports the use of the model for increasing Co thicknesses, which would become prohibitively expensive computationally if we were to insist upon obtaining raw DFT values.

Included in Table I are theoretically predicted values for the SESP corresponding to 0.5 ML C adatoms adsorbed on Co/Cu{100}. Such an experiment would be difficult to achieve from a practical perspective, but our work on oxygen and nitrogen adsorption gives us confidence in our theoretical methodology. Note that the effect of carbon is not significantly greater than that of nitrogen. A superficial glance at the calculated spin moments retained by the adsorbate and the uppermost cobalt layer could have suggested that carbon might have a much larger effect, as the adatom itself is antiferromagnetically coupled to the surface. The modeling technique presented here is therefore necessary for an accurate prediction of the adatom-influenced SESP, as inspection of the spin moments alone does not tell the full story.

In summary, the present work illustrates how the polarization of ferromagnetic thin films can be manipulated by adsorption of common atomic species. We have studied the effect of oxygen and nitrogen (as a function of Co film thickness) on the polarization of the ultrathin Co/Cu{100} system. Experimental SESP measurements have shown that oxygen has a very slight suppressive effect, whereas the nitrogen-adsorbed system was found to display an SESP lowered by around 20% compared to the clean surface. DFT results, when properly treated within an attenuation-based model, successfully reproduce the same behavior, and may therefore be used with confidence to predict the properties of systems for which experiments have yet to be performed. Crucially, our work serves uniquely to link the theoretical description of individual spin moments with an experimentally observable magnetic phenomenon.

D.S.D.G., K.P.K., D.K., and R.R. would like to thank the EPSRC for support. S.J.J. is grateful to The Royal Society for support. Computational resources were provided by the Cambridge High-Performance Computing Service. The authors wish to acknowledge their debt to the late Tony Bland, with whom this work was begun, and without whose continued input its completion has been immeasurably impoverished.

---

[1] C. A. F. Vaz, J. A. C. Bland, and G. Lauhoff, Rep. Prog. Phys. **71**, 056501 (2008).

[2] J. P. Velev, P. A. Dowben, E. Y. Tsymbal, S. J. Jenkins, and A. N. Caruso, Surf. Sci. Rep. **63**, 400 (2008).

[3] S. Pick, P. Legare, and C. Demangeat, Phys. Rev. B **75**, 195446 (2007).

[4] S. J. Jenkins, Surf. Sci. **600**, 1431 (2006).

[5] S. Pick, P. Legare, and C. Demangeat, J. Phys.: Condens. Matter **20**, 075212 (2008).

[6] R. Q. Wu and A. J. Freeman, J. Magn. Magn. Mater. **127**, 327 (1993).

[7] R. Q. Wu, A. J. Freeman, and G. B. Olson, Phys. Rev. B **47**, 6855 (1993).

[8] H. Huang and J. Hermanson, Phys. Rev. B **32**, 6312 (1985).

[9] S. R. Chubb and W. E. Pickett, Phys. Rev. Lett. **58**, 1248 (1987).

[10] C. Sorg, N. Ponpandian, M. Bernien, K. Baberschke, H. Wende, and R. Q. Wu, Phys. Rev. B **73**, 064409 (2006).

[11] S. Pick, Surf. Sci. **601**, 5571 (2007).

[12] S. Pick and H. Dreysse, Surf. Sci. **474**, 64 (2001).

[13] S. Yamagishi, S. J. Jenkins, and D. A. King, Surf. Sci. **543**, 12 (2003).

[14] Q. Ge, S. J. Jenkins, and D. A. King, Chem. Phys. Lett. **327**, 125 (2000).

[15] S. J. Jenkins, Q. Ge, and D. A. King, Phys. Rev. B **64**, 012413 (2001).

[16] C. L. Fu and A. J. Freeman, Phys. Rev. B **40**, 5359 (1989).

[17] S. Hope, E. Gu, M. Tselepi, M. E. Buckley, and J. A. C. Bland, Phys. Rev. B **57**, 7454 (1998).

[18] D. Matsumura, T. Yokoyama, K. Amemiya, S. Kitagawa, and T. Ohta, Phys. Rev. B **66**, 024402 (2002).

[19] S. van Dijken, R. Vollmer, B. Poelsema, and J. Kirschner, J. Magn. Magn. Mater. **210**, 316 (2000).

[20] R. Vollmer, T. Gutjahr-Loser, J. Kirschner, S. van Dijken, and B. Poelsema, Phys. Rev. B **60**, 6277 (1999).

[21] G. C. Burnett, T. J. Monroe, and F. B. Dunning, Rev. Sci. Instrum. **65**, 1893 (1994).

[22] M. Kittel, M. Polcik, R. Terborg, J. T. Hoeft, P. Baumgartel, A. M. Bradshaw, R. L. Toomes, J. H. Kang, D. P. Woodruff, M. Pascal, C. L. A. Lamont, and E. Rotenberg, Surf. Sci. **470**, 311 (2001).

[23] X. D. Liu, T. Iimori, K. Nakatsuji, and F. Komori, Appl. Phys. Lett. **88**, 133102 (2006).

[24] F. M. Leibsle, S. S. Dhesi, S. D. Barrett, and A. W. Robinson, Surf. Sci. **317**, 309 (1994).

[25] See EPAPS Document No. E-PRBMDO-80-079929 for further experimental details, as well as a discussion of the estimation of λ, N_0, and theoretical error bars. For more information on EPAPS, see http://www.aip.org/pubservs/epaps.html.

[26] D. Sekiba, S. Doi, K. Nakatsuji, and F. Komori, Surf. Sci. **590**, 138 (2005).

[27] W. Clemens, E. Vescovo, T. Kachel, C. Carbone, and W. Eberhardt, Phys. Rev. B **46**, 4198 (1992).

[28] K. P. Kopper, D. Kupper, R. Reeve, T. Mitrelias, J. A. C. Bland, J. Appl. Phys. **103**, 07C904 (2008).

[29] D. Briggs and M. P. Seah, *Practical Surface Analysis* (Wiley, Chichester, 1990), Vol. 1.

[30] D. Mauri, R. Allenspach, and M. Landolt, J. Appl. Phys. **58**, 906 (1985).

[31] F. O. Schumann, M. E. Buckley, and J. A. C. Bland, Phys. Rev. B **50**, 16424 (1994).

[32] P. Krams, F. Lauks, R. L. Stamps, B. Hillebrands, and G. Guntherodt, Phys. Rev. Lett. **69**, 3674 (1992).

[33] S. J. Clark, M. D. Segall, C. J. Pickard, P. J. Hasnip, M. J. Probert, K. Refson, and M. C. Payne, Z. Kristallogr. **220**, 567 (2005).

[34] D. Vanderbilt, Phys. Rev. B **41**, 7892 (1990).

[35] J. P. Perdew, J. A. Chevary, S. H. Vosko, K. A. Jackson, M. R. Pederson, D. J. Singh, and C. Fiolhais, Phys. Rev. B **46**, 6671 (1992).

[36] S. G. Louie, S. Froyen, and M. L. Cohen, Phys. Rev. B **26**, 1738 (1982).

[37] R. F. W. Bader, *Atoms in Molecules: A Quantum Theory* (Oxford University Press, Oxford, 1990).

[38] H. J. Monkhorst and J. D. Pack, Phys. Rev. B **13**, 5188 (1976).

[39] C. M. Schneider, P. Bressler, P. Schuster, J. Kirschner, J. J. de Miguel, and R. Miranda, Phys. Rev. Lett. **64**, 1059 (1990).